Lead Isotopic Constraints on the Provenance of Antarctic Dust and Relevant Atmospheric Circulation Patterns Prior to the Mid-Brunhes Event (~430 Kyr Ago)

Changhee Han
Korea Polar Research Institute
Laurie Burn
Curtin University
Paul Vallelonga
Curtin University
Soon Do Hur
Korea Polar Research Institute
Claude Boutron
Grenoble Alpes University
Sanghee Lee
Inha University
Sungmin Hong (smhong@inha.ac.kr)
Inha University

Research Article

Keywords: Pb, MBE, CWA, climatic

Posted Date: December 10th, 2020

DOI: https://doi.org/10.21203/rs.3.rs-120772/v1

Abstract

A lead (Pb) isotopic record, covering the two oldest glacial-interglacial cycles (~572 to 801 kyr ago), from the European Project for Ice Coring in Antarctica Dome C ice core provides isotopic evidence for the provenance of dust in deep Antarctic ice prior to the Mid-Brunhes Event (MBE), ~430 kyr ago, characterized by less warm interglacials. The isotopic signatures suggest Patagonia and central-western Argentina (CWA) as the primary sources of dust in central East Antarctica during both pre-MBE glacials and interglacials, in concert with an equatorward shift of the southern westerly winds (SWW). The contribution from extra-Antarctic volcanic emissions appears to be important for non-dust Pb in the pre-MBE interglacial and intermediate climates, most likely due to the reduction of wet removal efficiency with a weakening of the hydrologic cycle. Our results show a close coupling of the Southern Hemisphere atmospheric circulation patterns to climatic conditions prior to the MBE.

Introduction

The EPICA (European Project for Ice Coring in Antarctica) ice core drilled at Dome C (hereafter EDC) on the central East Antarctic Plateau (EAP) (75°06'S, 123°21'E, altitude 3,233 m above sea level) has provided unique archives of past climate changes over the last successive eight glacial-interglacial cycles back to Marine Isotope Stage (MIS) 20.2, ~ 800 kyr before present (B.P.)[1,2]. These eight climate cycles are characterized by a larger amplitude of climate variability with warmer interglacials after the Mid-Brunhes Event (MBE), ~ 430 kyr ago, compared to the earlier smaller climate changes with relatively cooler interglacials[2,3]. Together with the Antarctic temperature record, dust records from deep Antarctic ice cores are of particular interest as indicators of the sensitivity of atmospheric and surface conditions in lower latitude dust source regions to glacial-interglacial climate change, affecting the dust cycle at high latitudes[4,5]. However, the dust flux data alone cannot be used to ascertain to what extent the southern westerly winds (SWW) shifted in response to climate cycles, which is considered the underlying mechanism regulating glacial-interglacial variability of atmospheric CO_2[6–8]. A fundamental understanding of these paleo-atmospheric dynamics (that is, the latitudinal shift of the SWW) can be gained from study of climate-related dust provenance changes using isotopic evidence[9–16].

Strontium (Sr) and neodymium (Nd) isotopic compositions have been used for tracing the provenance of dust trapped in East Antarctic ice[9–13, 15,16]. Compared to Sr-Nd isotope provenance studies, however, determination of the provenance of Antarctic dust using lead (Pb) isotopes has been limited to very few studies[17–19], although Pb isotopes can be used as fingerprints to constrain dust sources and their evolution through space and time[20]. This is mainly because a reliable Pb isotope measurement in Antarctic deep ice cores remains an analytical challenge due to extremely low Pb concentrations at or below the picogram per gram (10^{-12} g g^{-1}) level and contaminants being brought to the outside of the deep ice cores that are inevitably drilled in holes filled with wall-retaining fluids[17,18,21].

Here we present the first Pb isotope ratios in the EDC ice, dated from ~ 572 to 801 kyr B.P., corresponding to the two oldest glacial-interglacial cycles prior to the MBE over the past ~ 800 kyr. These data allow us to compare variations in Pb isotopic composition between our new data and those previously obtained for the recent two climate cycles in the same ice core[18], thereby contributing to evaluations of dust provenance changes potentially linked to latitudinal shifts of the SWW between different climatic conditions before and after the MBE.

Results And Discussion

Pb and Ba concentrations and Pb isotopes

Elemental concentrations and Pb isotopic compositions measured in the innermost parts of individual samples are illustrated in Figure 1, together with the profiles of dust flux or deuterium (δD) as a function of the age of the ice, and all data are listed in Table S1. Figure 1 also shows published post-MBE data for the EDC ice core samples, dated from 2 kyr (MIS 1) to 220 kyr B.P. (MIS 7.3), by Vallelonga et al. (2010)[18].

Both the Pb and barium (Ba) concentrations show strong variability, with mean concentrations of Pb and Ba that are approximately 7 times higher during cold periods (δD < −405‰) than during interglacials (δD > −405‰) (Table S1), primarily dependent on the dust fluxes (Figures 1 and S1 of the supporting information). Note that glacial and interglacial periods were defined with a threshold δD value (−405‰), below which Antarctic temperature and dust flux show a clear correlation[5,23]. The Pb concentrations are positively well correlated with Ba (a conservative crustal reference element) during colder periods (δD < ~−420‰) with Pearson's correlation coefficient of 0.924 that is significant at the 0.01 significance level (2-tailed) (p = 0.01), while there is a lack of significant correlation during less cold periods (δD > ~−420‰) (Pearson's correlation coefficient of 0.344 at p = 0.117) (Figure S2). This reflects that dust was the main source of Pb in the EDC ice during cold climatic conditions[21,24].

Furthermore, the Pb concentrations show a sharp decrease when the δD values increase during colder glacials and remain very low when the δD values are above −420‰ (Figure S3). The very high Pb concentration (108 pg/g) in the deepest ice at 3,189.45 m (sample no. 40, ~801 kyr B.P., MIS 20.2) greatly exceeds the range of measured concentrations (< 20 pg/g) when the δD values are below −430‰ (Figures 1 and S3). Despite the stratigraphic continuity of multi-parametric climatic records above 3,200 m as described previously[2], the very high Pb content may suggest non-climate-related influences, possibly bedrock, and thus the sample is not included when interpreting climate signals. The Pb concentrations of sample nos. 25, 27, and possibly 20 also show apparent deviations from concentration levels during the intermediate and interglacial climatic stages (Figure S3), possibly due to Pb contributions from large volcanic eruptions[25].

The Pb isotope ratios vary from 1.1824 to 1.2332 for $^{206}Pb/^{207}Pb$ and from 2.4556 to 2.4939 for $^{208}Pb/^{207}Pb$ with mean values of 1.2022 and 2.4715, respectively (Table S1). Temporal changes in the pre-MBE $^{206}Pb/^{207}Pb$ ratios are less well characterized by temperature in Antarctica, while the post-MBE

values during 2–220 kyr B.P. show a general trend associated with climatic conditions with higher values during warm or less cold periods and lower values during very cold climatic stages (Figure 1). This difference may be partly due to larger age intervals (~90–250 years) integrated by individual pre-MBE samples relative to the post-MBE ones (~10–60 years), resulting in the smoothing of pre-MBE source-specific Pb isotopic signatures.

Comparison of Pb isotopic compositions before and after the MBE

Figure 2 shows the plot of $^{206}Pb/^{207}Pb$ versus $^{208}Pb/^{207}Pb$ for the pre-MBE and post-MBE glacials and interglacials. A perspective to consider is that natural Pb in Antarctic ice could originate from both dust and volcanoes[17,18,26]. An estimate of the dust contribution was made based on the Pb/Ba ratio of upper continental crust, ~0.03[18,27]. According to the fraction of Pb of dust origin, isotopic signatures in each sample were divided into dust-dominant Pb (> 60% with Pb/Ba < 0.05) and non-dust dominant Pb (< 60% with Pb/Ba > 0.05), as done for post-MBE isotopic signatures[18], which facilitated comparison of the isotopic compositions between the pre-MBE and post-MBE periods. A smaller estimated dust contribution indicates an increased non-dust (that is, volcanic) contribution.

In Figure 2, the pre-MBE Pb isotopic compositions show the distribution of the wide ranges of $^{206}Pb/^{207}Pb$ and $^{208}Pb/^{207}Pb$ with a general trend of less radiogenic compositions for dust-dominant Pb during glacial periods. Recently, Gili et al. (2016)[19] constrained well-defined potential source areas (PSAs) of dust in southern South America (SSA) by coupling Pb isotopic compositions in the EDC samples from Vallelonga et al. (2010)[18] with new Pb isotopic data from unexplored PSAs in SSA. In this study, however, Pb isotopic data by Vallelonga et al. (2010)[18] were not categorized into dust-dominant and non-dust dominant Pb for individual samples. In Figure 2, the post-MBE dust-dominant Pb isotopic signatures, combined with the PSAs fields defined by Gili et al. (2016)[19], indicate the central-western Argentina (CWA) and Patagonia as the primary sources of dust in East Antarctic ice during glacial periods. This is compatible with previous Sr-Nd isotopic constraints on the Antarctic dust provenance of Patagonia[9–16] and CWA[16] during the post-MBE glacials. Gili et al. (2016)[19] suggested the Puna-Altiplano Plateau (PAP) in the Andean Cordillera as the secondary source during glacials, based on a new perspective of Pb isotopic compositions falling on a distinct isotopic field of the PAP, characterized by higher $^{208}Pb/^{207}Pb$ relative to a given $^{206}Pb/^{207}Pb$ (Figure 2), consistent with the Sr-Nd isotopic constraints[15,16,28]. In Figure 2, part of the post-MBE glacial dust-dominant Pb isotopes also shows a shift toward the PAP field, supporting previous suggestions of the PAP provenance of glacial dust to the EAP.

Compared to the post-MBE glacial Pb isotopic compositions, the pre-MBE glacial dust-dominant Pb isotopes are characterized by lower radiogenic values (Table S2), exhibiting a tendency (except for sample no. 27, ~712 kyr B.P., Figure S4) to converge toward the partially overlapping field between Patagonia, Tierra del Fuego (TdF), and the southern and middle CWA (S-CWA and M-CWA, respectively) (Figure 2). Considering the Sr-Nd isotopic evidence for a dominant dust contribution from northern Patagonia relative to southernmost Patagonia (including TdF) in the post-MBE cold climates[16], the pre-

MBE glacial dust Pb isotopic compositions emerging within the overlapping field between Patagonia and TdF may be signals of northern Patagonia. As a result, the ratios distributed in a relatively narrow range between Patagonia, S-CWA, and M-CWA are thought to be a consequence of equally significant contributions from these potential dust sources to the EAP glacial dust during the pre-MBE glacials. The isotopic signature of sample no. 27 moves toward the most radiogenic McMurdo-Erebus volcanic field (Figure S4), likely associated with the effects of volcanic eruptions, probably Antarctic, as mentioned before (Figure S3). Interestingly, our new dust isotopic data show no dust transport from the PAP to the EAP during glacials prior to the MBE, which contrasts with previous observations for the post-MBE glacial dust as described above.

The pre-MBE interglacial dust-dominant Pb isotopes distribute within the Patagonian field (sample no. 11) or the overlapping field between Patagonia and TdF (sample nos. 3 and 34) (Figures 2 and S4), limiting the discrimination between the two potential sources. However, the isotopic ratios in the interglacial samples (nos. 1, 2, and 4) with relatively high fraction of dust Pb (~55 to 58%) show the signatures of Patagonia (Figures 2 and S4), providing insights into dominant dust supply from Patagonia during the pre-MBE interglacials. The isotopic composition plotted within the M-CWA field that partially overlaps with the southern Puna field is observed for sample no. 38 (Figure S4). Because the other pre-MBE interglacial and glacial isotopic data of dust-dominant Pb tend to fall on the Patagonian and CWA fields above the PAP compositional trend (Figure 2), this isotopic composition may reflect the M-CWA isotopic signature. A single data point would restrict the interpretation of the M-CWA dust provenance. However, the pre-MBE glacial dust-dominant isotopic compositions for sample nos. 26 and 30, with respective δD values of −407 and −411‰ near to the interglacial threshold δD value (−405‰) (Table S1), distribute within the M-CWA field (Figures 2 and S4). Taken together, our Pb isotope data suggest that the most important dust source was Patagonia, with an additional contribution from CWA, during the pre-MBE interglacials, although further studies with larger sample sizes are required to ensure the validity of our findings. For comparison, previous isotopic and geochemical studies suggested multiple sources of Patagonia[14,16,19,29], CWA[29], PAP[16,19], and Australia[13,14,30,31] for the post-MBE interglacial dust in the EAP ice.

A large difference in the isotopic compositions before and after the MBE is also observed for non-dust dominant Pb. In Figure 2, both the post-MBE glacial and interglacial isotopes of non-dust dominant Pb vary over a wide range of the mixing line between the non-radiogenic Patagonian dust field and the very radiogenic McMurdo-Erebus volcanic field. In contrast, the pre-MBE non-dust dominant Pb isotopes remained less radiogenic, except for four samples (sample nos. 20, 28, 29 and 40, Figure S4), relative to the post-MBE values (Figure 2 and Table S2). The distinctive non-radiogenic compositions of the pre-MBE volcanic Pb are likely due to extra-Antarctic volcanic contributions in association with the reduction of wet removal efficiency, coupled with an equatorward shift of the SWW belt (see next sections).

Dust provenance and its relevance to a shift of the SWW before the MBE

New isotopic evidence for Patagonian dust in the EDC ice core during the pre-MBE glacials indicates that Patagonia was the major dust source throughout the glacial periods over the past 800 kyr, consistent with previous Sr-Nd isotopic fingerprints of Patagonian glacial dust in the EAP ice prior to the MBE[13,28]. This suggests that the SWW remained over Patagonia (particularly northern Patagonia) under both pre-MBE and post-MBE Antarctic cold climates.

The dominance of Patagonian dust during glacial periods over the past 800 kyr would be linked to the glacial advances of the Northern and Southern Patagonian Ice Sheet (PIS), stretched from 37°S to 56°S, and the associated increase of fluvioglacial outwash deposits, allowing the enhanced dust entrainment associated with an increase in the vigour of atmospheric circulation[12,32,33]. Despite the lack of detailed records of glacier fluctuations in the PIS far back to MIS 20, the PIS glaciers likely reached its greater extent during glacial periods since the Great Patagonian Glaciation (~1 Ma ago)[34]. This suggests that the periodic expansion of the PIS glaciers in response to cold climate conditions, together with the northward expansion and intensification of the SWW[6,16,33,35], may have played an important role in the persistence of Patagonian dust provenance in the EAP ice during both the pre and post-MBE glacial periods. Along with an important role of the PIS, the persistent Patagonian glacial dust would be attributed in part to the larger increase of the exposed Argentine Shelf during the relative sea level low-stands between –80 m and –150 m below present sea level[12,33,36], when fine-grained shelf sediments were delivered from Patagonia[37], which in turn retained a dominant Patagonian dust signature[33].

Apart from a dominant and persistent Patagonian origin of glacial dust, our isotopic signatures indicate that CWA (S-CWA and M-CWA) emerges as an important dust supplier to the EAP during the pre-MBE glacials, as in the Sr-Nd isotopic constraints on the CWA origin of dust in recent glacial periods[16]. This suggests a northward extension of the SWW belt between northern Patagonia (39°–42°S) and CWA (27°–39°S), far north of its present position of the strong zonal winds between ~45°S and ~60°S[38], during both pre-MBE and post-MBE glacial periods. Although an equatorward displacement and strengthening of the SWW belt during glacial periods remains under debate (e.g., Kohfeld et al., 2013[39] and references therein), our explanation is consistent with the hypotheses that during the glacial conditions, an equatorward shift in the SWW was as large as 7–10° relative to its interglacial position[6] and the strengthening of the northern margin of the SWW occurred at 33°–40°S[35]. The northward shift of the northern edge of the SWW belt would have induced more vigorous northwesterly winds and the consequent increase in dust emissions over S-CWA and M-CWA[16], coupled with drier conditions in the SSA north of 40°S[39,40], enhancing the input of pre-MBE glacial dust from these areas to the EAP.

Another prominent feature of pre-MBE glacial isotopic compositions is the absence of a PAP dust signature, which contrasts with the hypothesis of its potential contribution during the post-MBE glacials, attributed to an equatorward movement of the subtropical westerly jet stream (SJT) over the PAP, a high elevation basin (~4,000 m a.s.l.)[15,16,19,28]. We attribute the non-contribution of PAP to the pre-MBE glacial dust in the EAP to environmental conditions that reduced either dust production in the PAP or efficient transfer of PAP dust to the EAP under cold climates of Antarctica prior to the MBE, probably linked to

shorter pre-MBE glacials than younger ones, which consequently reduced the dust productivity in the major dust sources at lower latitudes in the Southern Hemisphere[41]. Although hypothetical, a less pronounced increase in the EDC glacial dust fluxes prior to the MBE (notably MIS 16, 18 and 20) relative to the post-MBE glacials (e.g., MIS 8 and 10), as noted previously[36], would be partly due to the absence of any glacial dust supply from PAP (Figure 1), assuming the similarity of a strengthening of SSA PSAs and the transport efficiency of dust from SSA PSAs to the EAP between the pre-MBE and post-MBE glacial conditions[5]. A tentative assessment of the relative dust contribution in the EDC glacial ice, using the Nd isotopic composition between a Patagonian and a PAP end-member, suggested that when glacial dust input to the EAP increased, the contribution from Patagonia decreased, while the contribution from a secondary source, PAP, increased, and vice versa, during Pleistocene glacial times[28], supporting the above hypothesis.

During the pre-MBE interglacials, our Pb isotopic signatures characterize a dominance of dust from Patagonia with the existence of additional input of dust from CWA, suggesting favorable atmospheric circulation for the persistence of dust production and transfer of dust from these source regions. Patagonia is situated in a large region in SSA, extending from ~39°S down to the southern tip (~55°S) of South America including TdF in the southernmost part, and the climate is currently controlled by the dynamics of the SWW belt[16]. Satellite and surface observations near the sources and in Antarctica, combined with model simulations, identified modern dust transport from the southern Patagonia and TdF as far south as ~55°S to the EAP in austral summer[42]. Compared to this current feature of the southernmost dust source, the dominant contribution of dust from Patagonia, excluding TdF, during the pre-MBE interglacials may reflect slightly northward shifted SWW belt under cooler pre-MBE interglacial climates. Meanwhile, the presence of dust from CWA suggests an influence of the SWW belt exerting over this region, following a systematic movement of the SWW with the mean climate[6,43]. Today, the atmospheric circulation in CWA is dominated by the northeasterly wind in austral summer and northwesterly wind in austral winter[44], and by the katabatic wind (called Zonda wind), an extremely dry wind blowing from west to east, injecting dust aloft, from May to August[16]. Taken together, our isotopic constraints on the provenance of dust in the pre-MBE interglacial ice can be explained by a northward shift and/or extension of the SWW belt in response to cooler pre-MBE interglacial climates relative to the post-MBE interglacials. This may have enhanced dust supply and strong wind uptake as a consequence of more frequent cyclonic influence and more steady zonal winds in SSA as in the case for winter conditions in the current climate[45]. Interestingly, the EDC ice core record shows a substantial increase of dust fluxes during cooler pre-MBE interglacials (MIS 15.1, 15.5, 17.3 and 19.3), compared to the warmer post-MBE interglacials (MIS 1 and 5.5)[3,5]: the average (± SD) dust flux during the pre-MBE MIS 15.1, 15.5, 17.3 and 19.3 interglacials is 0.85 ± 0.61 mg/m^2/yr, which is ~ 2 times the average flux (0.45 ± 0.20 mg/m^2/yr) of the post-MBE MIS 1 and 5.5 interglacials. Furthermore, the EDC interglacial ice CO_2 levels prior to the MBE were ~30–40 ppm lower than those after the MBE[46,47]. This may be partly related to the weakened strength of the Antarctic Circumpolar Current in response to a northward shift in the mean position of the SWW, resulting in reduced ventilation of respired CO_2 in the deep ocean to the

atmosphere[6,7]. However, any speculation must be treated cautiously due to the lack of a comprehensive understanding of processes and mechanisms for the lower interglacial CO_2 levels prior to the MBE[48].

Pre-MBE volcanic isotopic signatures and atmospheric implications

An interesting difference in the Pb isotopic signatures between the pre-MBE and post-MBE periods is observed when the $^{206}Pb/^{207}Pb$ ratios are plotted as a function of relative dust-Pb proportions (Figure 3). The post-MBE $^{206}Pb/^{207}Pb$ ratios with a dust-Pb fraction of < 60%, reflecting an increase of volcanic Pb source, show a clear compositional trend moving toward the most radiogenic McMurdo-Erebus volcanic field. This trend was previously interpreted as a result of an increasing mixture of volcanic Pb from degassing volcanoes within Antarctica[18,19]. For comparison, the pre-MBE $^{206}Pb/^{207}Pb$ ratios show no distinct increasing trend (except for sample nos. 20, 28, 29 and 40) (Figures 3 and S5), approaching the isotopic compositions characterized by extra-Antarctic volcanoes north of 60°S (Figure S6).

A possible clue to explain this difference can be seen from the climatic conditions for pre-MBE and post-MBE individual data. In Figure 3, the post-MBE volcanic Pb appears to increase during very cold ($\delta D < -425‰$) or intermediate ($-405‰ < \delta D < -425‰$) climates, while the pre-MBE samples typically show an increasing volcanic contribution mostly during warm ($\delta D > -405‰$) or intermediate climates. Note that the pre-MBE samples (nos. 19, 24 and 25) classified into the intermediate climate have δD values between −408 and −411‰, (Table S1). Discrete volcanic tephra layers identified in the EDC ice core do not match with the post-MBE samples[18,49] and they tend to disappear in the EDC ice older than 358 kyr BP, probably due to the variations in the frequency of large volcanic eruptions[50]. This suggests no impact of sporadic explosive volcanic eruptions on the compositional trend of volcanic Pb isotopes observed for the pre-MBE periods, except for sample nos. 20, 25 and 27, showing abnormally enhanced Pb concentrations, probably due to large volcanic eruptions (Figure S3). The trend of climate-related pre-MBE $^{206}Pb/^{207}Pb$ ratios does not change after excluding these three data points (Figure S5).

Given the above, the a priori guess would be that the dominant isotopic signatures of Antarctic volcanoes during the post-MBE glacials are likely due to a stronger dynamical isolation of the polar vortex area over Antarctica under cold climate conditions[12], reducing the advection of extra-Antarctic volcanic degassing Pb to the EAP through the low levels of troposphere, which differs from the dust transport from South American sources via the upper tropospheric pathways[5,23]. Interestingly, the pre-MBE isotopic compositions for sample nos. 28 and 29 with much lower δD values (−438‰ and −422‰, respectively) show an approach to the McMurdo-Erebus volcanic signature (Figure S5), supporting the above speculation. On the other hand, the lack of extra-Antarctic volcanic Pb signature during the post-MBE interglacials is most likely due to the enhanced en route wet removal resulting from either a more intense hydrological cycle[5,23,39,40] or the poleward shift of intense cyclones in the mid-latitudes under warm climate conditions[51]. This hypothesis, however, contradicts a previous study proposing that high super-chondritic (volcanic) platinum (Pt) and iridium (Ir) fluxes in the EAP during the post-MBE interglacials (MIS 1 and 5) were probably due to the enhanced advection of air masses from lower latitudes to the EAP

according to a weakened polar vortex[52]. This contradiction may arise from differences in the removal efficiency of individual volcanogenic metals from the atmosphere primarily via wet deposition processes of within-cloud scavenging and below-cloud scavenging (wash-out). The modeling study of volcanic emissions showed that volcanic $PbCl_2$, a highly soluble species enriched in degassing volcanic emissions, decreased exponentially in the atmosphere with the distance from the volcano due to the rapid wet deposition[53]. In contrast, refractory and chemically inert Ir and Pt that are enriched in volcanic emissions in association with the high fluorine content, compose water insoluble fluoride species (e.g., iridium hexafluoride, IrF_6)[54], which would have the potential for further atmospheric transport over long distances. Recent studies identified well-defined Pt and Ir peaks in the volcanic layers of Antarctic and Greenland snow deposits without Pb enrichments coincident with these peaks[24,55,56], supporting our hypothesis.

As a result, we can infer that extra-Antarctic volcanic Pb signatures in the pre-MBE interglacial climates are most likely related to a longer lifetime for volcanic aerosols from degassing volcanoes, associated with the reduction of wet removal efficiency. Together with a prolonged lifetime of volcanic aerosols, a northward shift and/or extension of the SWW belt during cooler pre-MBE interglacials could have enhanced an advection of volcanic Pb from volcanoes outside Antarctica to the EAP. Our results point to a substantial weakening of the hydrologic cycle in line with cooler sea surface temperature of the Southern Ocean during pre-MBE lukewarm interglacials relative to the post-MBE interglacials[8,57].

Conclusions

New Pb isotope data for the oldest part of the EDC ice core provide the first evidence for Patagonia and CWA as the persistent sources of East Antarctic dust during both cold glacial and lukewarm interglacial climates over the two oldest glacial-interglacial cycles prior to the MBE. Combined with implications of the isotopic signatures for an increased advection of extra-Antarctic volcanic Pb to the EAP during pre-MBE interglacial and intermediate climates, our isotopic data suggest the emergence of CWA as an important potential dust supplier to the EAP during the pre-MBE interglacials, which is most likely related to a northward shift and/or extension of the SWW belt in combination with a weakened hydrologic cycle as a result of cooler climatic conditions during the corresponding periods relative to the post-MBE interglacials. Our findings highlight a sensitive feature for changes in the position of the SWW belt and hydrologic cycle intensity in response to pre-MBE climate cycles. Further work is necessary to better understand the modes of variability of the southern climatic system on different time-scales of climate changes.

Methods

Ice core samples and decontamination procedure

We have analyzed 40 samples obtained from 30 core sections of the 3,260-m EDC ice core, with depths from 2,973.91 (572,800 yr B.P., MIS 15.1) to 3,189.45 m (801,590 yr B.P., MIS 20.2)[58] (Figure 1). The depth and estimated age of each sample are given in Table S1 in the supporting information. Each of the 30 ice core sections (55 cm in length and 5 cm in radius) from the 3,260-m EPICA Dome C ice core, drilled in a fluid-filled hole[1], was mechanically decontaminated using an acid-cleaned polyethylene lathe and ultraclean working procedures at the Korea Polar Research Institute (KOPRI)[21,59]. These involve the chiseling of successive layers of ice in progression from the contaminated outside toward the center of the section using acid-cleaned ultraclean stainless steel chisels. An external ~2 mm thick layer of the most highly contaminated ice was scraped away before decontaminating. All the equipment used during the entire operation was extensively acid-cleaned prior to use and the chiseling was performed inside a laminar flow class 100 clean bench located in a cold room at –15°C. After the chiseling was completed, the inner core was then cut into two consecutive 20 cm long parts when the whole inner core was available. Altogether, 40 samples were analyzed for this study. Each sample was melted at room temperature in ultra-clean wide mouth low-density polyethylene (LDPE) 1 L bottles within a class 100 clean bench inside a class 10,000 clean room at KOPRI. About 10 mL aliquots were taken into acid-cleaned ultraclean 15 mL LDPE bottles and were then transported frozen to Curtin University in Perth, Australia, for Pb and Ba concentrations and Pb isotope analysis.

Mass spectrometry

The procedures of sample processing and analysis by thermal ionization mass spectrometry (TIMS) have been described in detail by Burn et al. (2009)[60]. Briefly, the ice samples were melted and aliquots of ~1 to 10 g were transferred to PFA Teflon beakers, depending on the expected Pb contents based on the preliminary results of inductively coupled plasma sector field mass spectrometry (ICP-SFMS) analysis. A mixture of HNO_3/HF/H_3PO_4 and a $^{205}Pb/^{137}Ba$ isotopically enriched spike solution were then added before the sample and tracer mixture were evaporated to dryness. The addition of the enriched isotopes ^{205}Pb and ^{137}Ba enables the quantities of Pb and Ba to be accurately determined by isotope dilution mass spectrometry (IDMS)[60]. The samples were loaded onto a degassed (4 A, 30 min), zone-refined rhenium filament (99.999% Re, 0.7 mm wide and 0.04 mm thick, H. Cross Company) with 4 µL of silica-gel and again evaporated to dryness. Prior to mounting the sample and silica-gel mixture, the filament was acid-cleaned using 7 µL of 1% Fisher “Optima” grade ultrapure HNO_3 at 1.5 A. Samples were simultaneously analyzed for Pb and Ba concentrations using IDMS and Pb isotopes using a TRITON (Thermo Scientific) TIMS[60]. All ion beams were measured with a secondary electron multiplier (SEM), collecting ~300 isotope ratios per sample. The accuracy of the Pb and Ba concentrations is estimated to be ±10% (95% confidence interval), attributed mainly to the accuracy of dispensing the spike into the sample[60]. Two procedural blanks and two or more reference material samples containing a ~100 pg of NIST 981 SRM Pb isotopic standard were analyzed together with each batch of up to ~21 samples for quality control and monitoring of instrumental mass fractionation[60]. A correction for isotopic fractionation of 0.11 ± 0.08% per mass unit was applied to the measured ratios. Pb isotope ratio uncertainties at 95% confidence interval (Table S1, supporting information) are associated with the

sample analysis, the isotopic composition of the Pb blank and the instrumental mass fractionation correction.

Validation methodology for decontamination procedures

Although careful elimination of the significant contamination from the outside of the core sections were performed by mechanical chiseling as describe above, changes in the measured Pb and Ba concentrations and Pb isotope ratios as a function of radius from the outside to the inside of the core were investigated for the selected core sections to check the efficiency of the decontamination. Examples of such concentrations and isotope profiles are shown in Figure S7 of the supporting information. In all cases, concentrations and isotope ratios are observed to level off at well-established plateau values in the central parts of the sections, indicating no transfer of the outside contamination to the inner part of the core.

Declarations

Acknowledgments

The EDC δD and dust data sets described in this article are available at http://www.ncdc.noaa.gov/data-access/paleoclimatology-data/datasets/ice-core and http://doi.pangaea.de/10.1594/PANGAEA.779310, respectively. We wish to thank all the participants in the field at Dome C, East Antarctica. This work is a contribution to the European Project for Ice Coring in Antarctica (EPICA), a joint ESF (European Science Foundation)/EC scientific program (EPICA-MIS), funded by the European Commission and by national contributions from Belgium, Denmark, France, Germany, Italy, the Netherlands, Norway, Sweden, Switzerland, and the United Kingdom. This work was supported by research grants from the Korea Polar Research Institute (PE20190) and the Basic Science Research Program through the National Research Foundation of Korea (NRF) funded by the Ministry of Education, Science and Technology (NRF-2018R1A2B2006489). This work was also supported by the Villum Investigator Project IceFlow (NR. 16572). This paper is dedicated to the memory of late Professor Kevin Rosman, who pioneered the study of Pb isotopes in polar snow and ice.

Author Contributions

S.H. designed this study and drafted the manuscript. C.H. and S.D.H conducted the ultraclean decontamination procedures and C.H., L.J.B., P.V. performed the analyses of Pb isotopes and Pb and Ba concentrations. P.V., C.F.B., and S.L. reviewed the data. All authors contributed to the interpretation and the writing of the manuscript.

Competing Interests

The authors declare no completing interests.

Data Availability Statement

Data presented in this study are available in Table S1 and will be archived at the World Data Center PANGAEA (https://www.pangaea.de).

References

1. EPICA community members. Eight glacial cycles from an Antarctic ice core. *Nature* **429**, 623–628 (2004).
2. Jouzel, J. *et al*. Orbital and millennial Antarctic climate variability over the past 800,000 years. *Science* **317**, 793–796 (2007).
3. Masson-Delmotte, V. *et al*. EPICA Dome C record of glacial and interglacial intensities. *Quat. Sci. Rev.* <background-color:#FFCC66;bu>29</background-color:#FFCC66;bu>, 113–128 (2010).
4. Yung, Y. L., Lee, T., Wang, C. –H. & Shieh, Y. –T. Dust: A diagnostic of the hydrologic cycle during the last glacial maximum. *Science* **271**, 962–963 (1996).
5. Lambert, F. *et al*. Dust-climate couplings over the past 800,000 years from the EPICA Dome C ice core. *Nature* **452**, 616–619 (2008).
6. Toggweiler, J. R., Russell, J. & Carson, S. R. Midlatitude westerlies, atmospheric CO<background-color:#CCCCFF;usub>2</background-color:#CCCCFF;usub>, and climate change during the ice ages. *Paleoceanography* <background-color:#FFCC66;bu>21</background-color:#FFCC66;bu>, PA2005 (2006).
7. Menviel, L. *et al*. Southern Hemisphere westerlies as a driver of the early deglacial atmospheric CO<background-color:#CCCCFF;usub>2</background-color:#CCCCFF;usub> rise. *Nat. Commun.* <background-color:#FFCC66;bu>9</background-color:#FFCC66;bu>, 2503 (2018).
8. Lamy, F. *et al*. Precession modulation of the South Pacific westerly wind belt over the past million years. *Proc. Natl. Acad. Sci.* **112**, 1–6 (2019).
9. Grousset, F. E. *et al*. Antarctic (Dome C) ice-core dust at 18 k.y. B.P.: Isotopic constraints on origins. *Earth Planet. Sci. Lett.* **111**, 175–182 (1992).
10. Basile, I. *et al*. Patagonian origin of glacial dust deposited in East Antarctica (Vostok and Dome C) during glacial stages 2, 4 and 6. *Earth Planet. Sci. Lett.* <background-color:#FFCC66;bu>146</background-color:#FFCC66;bu>, 573–589 (1997).
11. Smith, J. *et al*. Isotopic constraints on the source of Argentinian loess – with implications for atmospheric circulation and the provenance of Antarctic dust during recent glacial maxima. *Earth Planet. Sci. Lett.* <background-color:#FFCC66;bu>212</background-color:#FFCC66;bu>, 181–196 (2003).
12. Delmonte, B. *et al*. Comparing the Epica and Vostok dust records during the last 220,000 years: stratigraphical correlation and provenance in glacial periods. *Earth Sci. Rev.* **66**, 63–87 (2004).
13. Delmonte, B. *et al*. Aeolian dust in East Antarctica (EPICA-Dome C and Vostok): Provenance during glacial ages over the last 800 kyr. *Geophys. Res. Lett.* **35**, L07703 (2008).

14. Marino, F. *et al*. Defining the geochemical composition of the EPICA Dome C ice core dust during the last glacial-interglacial cycle. *Geochem. Geophys. Geosyst.* <background-color:#FFCC66;bu>9</background-color:#FFCC66;bu>, 1–11 (2008).
15. Gaiero, D. M. Dust provenance in Antarctic ice during glacial periods: From where in southern South America? *Geophys. Res. Lett.* **34**, L17707 (2007).
16. Gili, S. *et al*. Glacial/interglacial changes of Southern Hemisphere wind circulation from the geochemistry of South American dust. *Earth Planet. Sci. Lett.* **469**, 98–109 (2017).
17. Vallelonga, P., Gabrielli, P., Rosman, K. J. R., Barbante, C. & Boutron, C.F. A 220 kyr record of Pb isotopes at Dome C Antarctica from analyses of the EPICA ice core. *Geophys. Res. Lett.* **32**, L01706 (2005).
18. Vallelonga, P. *et al*. Lead isotopic compositions in the EPICA Dome C ice core and Southern Hemisphere Potential Source Areas. *Quat. Sci. Rev.* **29**, 247–255 (2010).
19. Gili, S. *et al*. Provenance of dust to Antarctica: A lead isotopic perspective. *Geophys. Res. Lett.* **43**, 2291–2298 (2016).
20. Han, C. *et al*. High-resolution isotopic evidence for a potential Saharan provenance of Greenland glacial dust. *Sci. Rep.* <background-color:#FFCC66;bu>8</background-color:#FFCC66;bu>, 15582 (2018).
21. Hong, S. *et al*. Climate-related variations in lead concentrations and sources in Vostok Antarctic ice from 65,000 to 240,000 years BP. *Geophys. Res. Lett.* <background-color:#FFCC66;bu>30</background-color:#FFCC66;bu>, 2138 (2003).
22. Lisiecki, L. E. & Raymo, M. E. A Pliocene-Pleistocene stack of 57 globally distributed benthic $\delta^{18}O$ records. *Paleoceanography* **20**, 1–17 (2005).
23. Petit, J. R. & Delmonte, B. A model for large glacial-interglacial climate-induced changes in dust and sea salt concentrations in deep ice cores (central Antarctica): palaeoclimatic implications and prospects for refining ice core chronologies. *Tellus* <background-color:#FFCC66;bu>61B</background-color:#FFCC66;bu>, 768–790 (2009).
24. Marteel, A. *et al*. Changes in atmospheric heavy metals and metalloids in Dome C (East Antarctica) ice back to 672.0 kyr BP (Marine Isotopic Stages 16.2). *Earth Planet. Sci. Lett.* <background-color:#FFCC66;bu>272</background-color:#FFCC66;bu>, 579–590 (2008).
25. Chang, C. *et al*. Persistent Pb pollution in central East Antarctic snow: A retrospective assessment of sources and control policy implications. *Environ. Sci. Technol.* **50**, 12,138–12,145 (2016).
26. Hinkley, T. Lead (Pb) in old Antarctic ice: Some from dust, some from other sources. *Geophys. Res. Lett.* **34**, 1–4 (2007).
27. Wedepohl, K. H. The composition of the continental crust. *Geochim. Cosmochim. Acta* **59**, 1217–1232 (1995).
28. Delmonte, B. *et al*. Geographic provenance of aeolian dust in East Antarctica during Pleistocene glaciations: preliminary results from Talos Dome and comparison with East Antarctic and new

Andean ice core data. *Quat. Sci. Rev.* **29**, 256–264 (2010).

29. Paleari, C. I. *et al*. Aeolian dust provenance in central East Antarctica during the Holocene: Environmental constraints from single-grain Raman Spectroscopy. *Geophys. Res. Lett.* **46**, 1–12 (2019).
30. Revel-Rolland, M. *et al*. Eastern Australia: a possible source of dust in East Antarctica interglacial ice. *Earth Planet. Sci. Lett.* **249**, 1–13 (2006).
31. De Deckker, P., Norman, M., Goodwin, I. D., Wain, A. & Gingele, F. X. Lead isotopic evidence for an Australian source of aeolian dust to Antarctica at times over the last 170,000 years. *Palaeogeogr. Palaeoclimatol. Palaeoecol.* <background-color:#FFCC66;bu>285</background-color:#FFCC66;bu>, 205–223 (2010).
32. Sugden, D. E., McCulloch, R. D., Bory, A. J. –M. & Hein, A. S. Influence of Patagonian glaciers on Antarctic dust deposition during the last glacial period. *Nat. Geosci.* **29**, 281–285 (2009).
33. Kaiser, J. & Lamy, F. Links between Patagonian Ice Sheet fluctuations and Antarctic dust variability during the last glacial period (MIS 4 – 2). *Quat. Sci. Rev.* **29**, 1464–1471 (2010).
34. Rabassa, J., Coronato, A. & Martínez, O. Late Cenozoic glaciations in Patagonia and Tierra del Fuego: an updated review. *Biol. J. Linn. Soc. Lond.* **103**, 316–335 (2011).
35. Lamy, F. *et al*. Glacial reduction and millennial-scale variations in Drake Passage throughflow. *Proc. Natl. Acad. Sci.* **112**, 13496–13501 (2015).
36. Wolff, E. W. *et al*. Changes in environment over the last 800,000 years from chemical analysis of the EPICA Dome C ice core. *Quat. Sci. Rev.* <background-color:#FFCC66;bu>29</background-color:#FFCC66;bu>, 285–295 (2010).
37. Gaiero, D. M., Probst, J. –L., Depetris, P. J., Bidart, S. M. & Leleyter, L. Iron and other transition metals in Patagonian riverborne and windborne materials: Geochemical control and transport to the southern South Atlantic Ocean. *Geochim. Cosmochim. Acta* <background-color:#FFCC66;bu>67</background-color:#FFCC66;bu>, 3603–3623 (2003).
38. Garreaud, R. D., Vuille, M., Compagnucci, R. & Marengo, J. Present-day South American climate. *Palaeogeogr. Palaeoclimatol. Palaeoecol.* **281**, 180–195 (2009).
39. Kohfeld, K. E. *et al*. Southern Hemisphere westerly wind changes during the Last Glacial Maximum: paleo-data synthesis. *Quat. Sci. Rev.* **68**, 76–95 (2013).
40. Clark, P. U. *et al*. Global climate evolution during the last deglaciation. *Proc. Natl. Acad. Sci.* **109**, E1134–E1142 (2012).
41. Lamy, F. *et al*. Increased dust deposition in the Pacific Southern Ocean during glacial periods. *Science* **343**, 403–407 (2014).
42. Gassó, S. *et al*. A combined observational and modeling approach to study modern dust transport from the Patagonia desert to East Antarctica. *Atmos. Chem. Phys.* **10**, 8287–8303 (2010).
43. Lamy, F. *et al*. Holocene changes in the position and intensity of the southern westerly wind belt. *Nat. Geosci.* **3**, 695–699 (2010).

44. Zárate, M. A. & Tripaldi, A. The aeolian system of central Argentina. *Aeolian Res.* **3**, 401–417 (2012).
45. Lambert, F., Bigler, M., Steffensen, J. P., Hutterli, M. & Fischer, H. Centennial mineral dust variability in high-resolution ice core data from Dome C, Antarctica. *Clim. Past* <background-color:#FFCC66;bu>8</background-color:#FFCC66;bu>, 609–623 (2012).
46. Lüthi. D. *et al*. High-resolution carbon dioxide concentration record 650,000–800,000 years before present. *Nature* <background-color:#FFCC66;bu>453</background-color:#FFCC66;bu>, 379–382 (2008).
47. Bereiter, B. *et al*. Revision of the EPICA Dome C CO<background-color:#CCCCFF;usub>2</background-color:#CCCCFF;usub> record from 800 to 600 kyr before present. *Geophys. Res. Lett.* <background-color:#FFCC66;bu>42</background-color:#FFCC66;bu>, 542–549 (2014).
48. Bouttes, N., Swingedouw, D., Roche, D. M., Sanchez-Goni, M. F. & Crosta, X. Response of the carbon cycle in an intermediate complexity model to the different climate configurations of the last nine interglacials. *Clim. Past* **14**, 239–253 (2018).
49. Narcisi, B., Petit, J. R., Delmonte, B., Basile-Doelsch, I. & Maggi, V. Characteristics and sources of tephra layers in the EPICA-Dome C ice record (East Antarctica): Implications for past atmospheric circulation and ice core stratigraphic correlations. *Earth Planet. Sci. Lett.* **239**, 253–265 (2005).
50. Narcisi, B., Petit, J. R. & Delmonte, B. Extended East Antarctic ice-core tephrostratigraphy. *Quat. Sci. Rev.* **29**, 21–27 (2010).
51. Tamarin, T. & Kaspi, Y. The poleward shift of storm tracks under global warming: A Lagrangian perspective. *Geophys. Res. Lett.* <background-color:#FFCC66;bu>44</background-color:#FFCC66;bu>, 10,666–10,674 (2017).
52. Gabrielli, P. *et al*. A climatic control on the accretion of meteoric and super-chondritic iridium-platinum to the Antarctic ice cap. *Earth Planet. Sci. Lett.* <background-color:#FFCC66;bu>250</background-color:#FFCC66;bu>, 459–469 (2006).
53. Pfeffer, M., Langmann, B. & Graf, H. –F. Atmospheric transport and deposition of Indonesian volcanic emissions. *Atmos. Chem. Phys.* **6**, 2525–2537 (2006).
54. Zoller, W. H., Parrington, J. R. & Kotra, J. M. P. Iridium enrichment in airborne particles from Kilauea Volcano. *Science* **222**, 1118–1121 (1983).
55. Gabrielli, P. *et al*. Siderophile metal fallout to Greenland from the 1991 winter eruption of Hekla (Iceland) and during the global atmospheric perturbation of Pinatubo. *Chem. Geol.* <background-color:#FFCC66;bu>255</background-color:#FFCC66;bu>, 78–86 (2008).
56. Soyol-Erdene, T. –O., Hur, Y., Hong, S. & Hur, S. D. A 50-year record of platinum, iridium, and rhodium in Antarctic snow: Volcanic and anthropogenic sources. *Environ. Sci. Technol.* <background-color:#FFCC66;bu>45</background-color:#FFCC66;bu>, 5929–5935 (2011).
57. Schaefer, G. *et al*. Planktonic foraminiferal and sea surface temperature record during the last 1 Myr across the Subtropical Front, Southwest Pacific. *Mar. Micropaleontol.* <background-color:#FFCC66;bu>5</background-color:#FFCC66;bu>4, 191–212 (2005).

58. Veres, D. *et al*. The Antarctic ice core chronology (AICC2012): an optimized multi-parameter and multi-site dating approach for the last 120 thousand years. *Clim. Past* **9**, 1733–1748 (2013).
59. Hur, S. D. *et al*. Climate-related variations in atmospheric Sb and Tl in the EPICA Dome C ice (East Antarctica) during the past 800,000 years. *Global Biogeochem. Cycles* **27**, 930–940 (2013).
60. Burn, L. J. *et al*. An ultra-clean technique for accurately analyzing Pb isotopes and heavy metals at high spatial resolution in ice cores with sub-pg g^{-1} Pb concentrations. *Anal. Chim. Acta* **634**, 228–236 (2009).

Figures

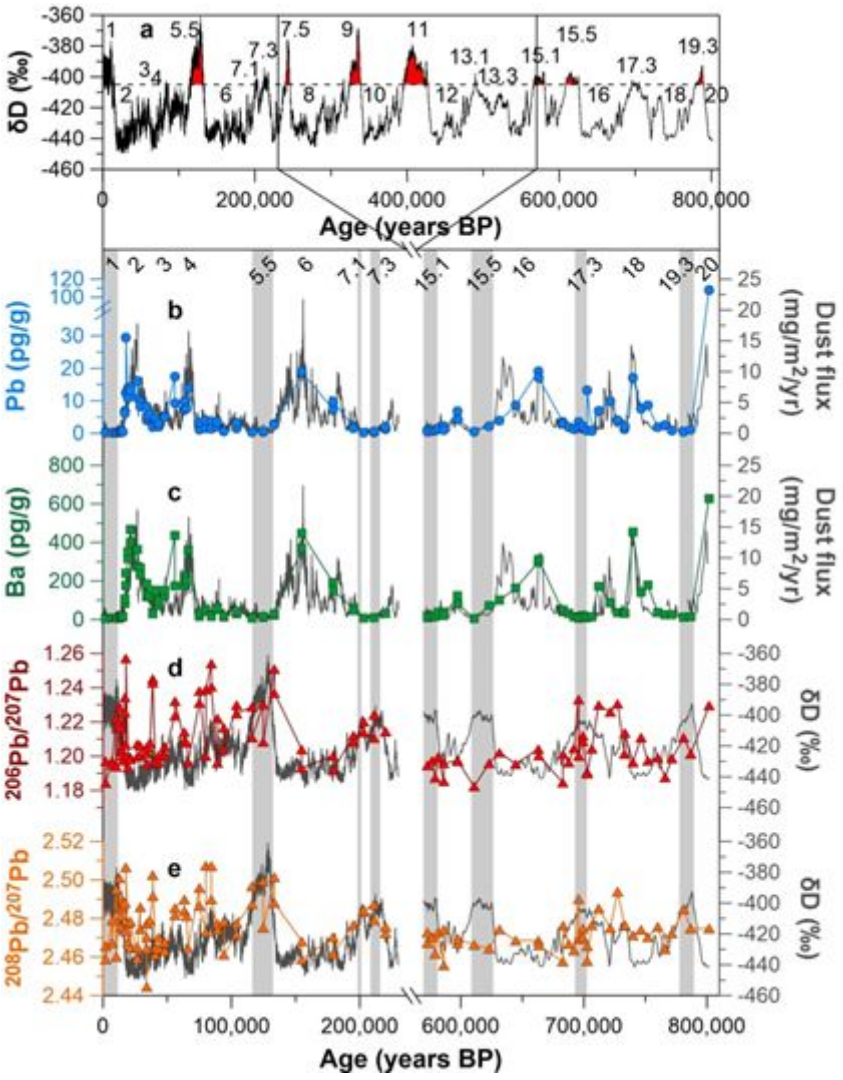

Figure 1

Changes in Pb and Ba concentrations, and Pb isotopic compositions from the EDC ice core. Also included are previously published data from the EDC ice core during the reporting period from 2 kyr (MIS 1) to 220 kyr B.P. (MIS 7.3)18. (a) The full EDC δD (Antarctic temperature proxy) profile2 with Marine Isotope Stage (MIS) numbers22. (b, c) Changes in Pb and Ba concentrations and their deposition fluxes. Flux of dust in

the EDC ice core5 is shown as a gray solid line for comparison. (d, e) Changes in 206Pb/207Pb and 208Pb/207Pb ratios. The δD record in the EDC ice core is shown as a gray solid line for comparison. The vertical grey bars represent the interglacial periods when the δD values are above −405‰.

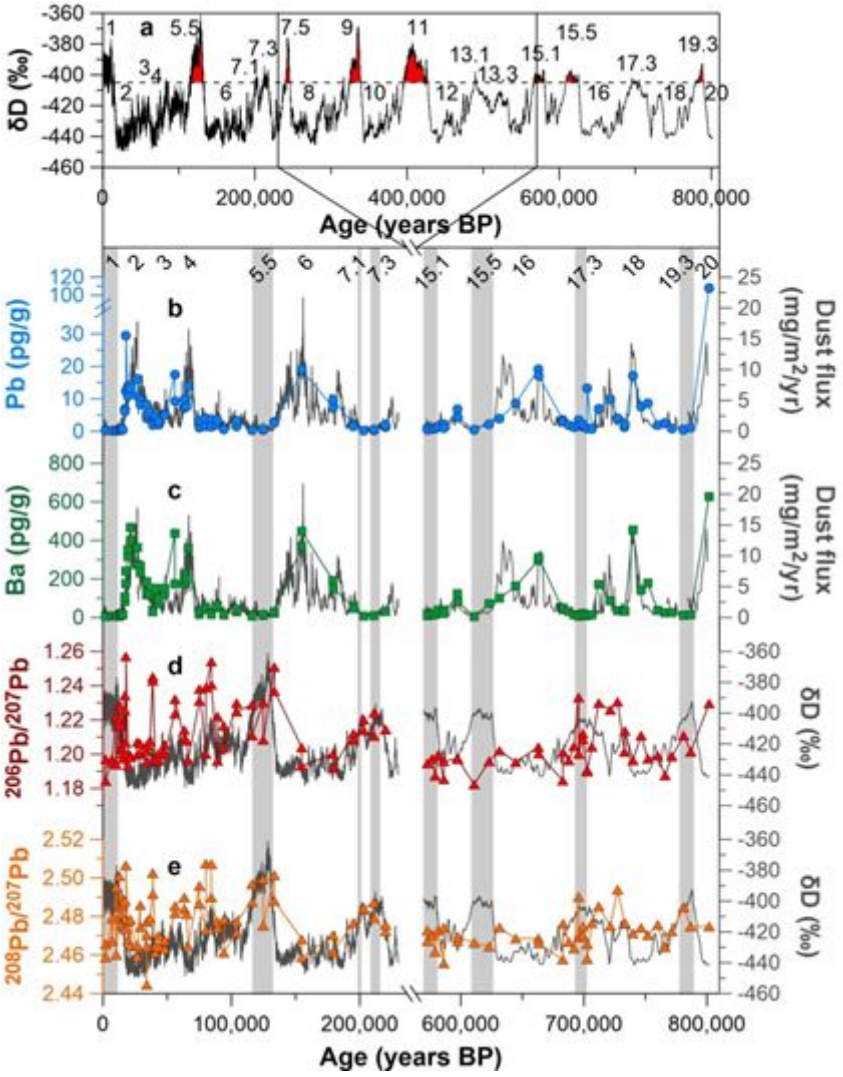

Figure 1

Changes in Pb and Ba concentrations, and Pb isotopic compositions from the EDC ice core. Also included are previously published data from the EDC ice core during the reporting period from 2 kyr (MIS 1) to 220 kyr B.P. (MIS 7.3)18. (a) The full EDC δD (Antarctic temperature proxy) profile2 with Marine Isotope Stage (MIS) numbers22. (b, c) Changes in Pb and Ba concentrations and their deposition fluxes. Flux of dust in the EDC ice core5 is shown as a gray solid line for comparison. (d, e) Changes in 206Pb/207Pb and 208Pb/207Pb ratios. The δD record in the EDC ice core is shown as a gray solid line for comparison. The vertical grey bars represent the interglacial periods when the δD values are above −405‰.

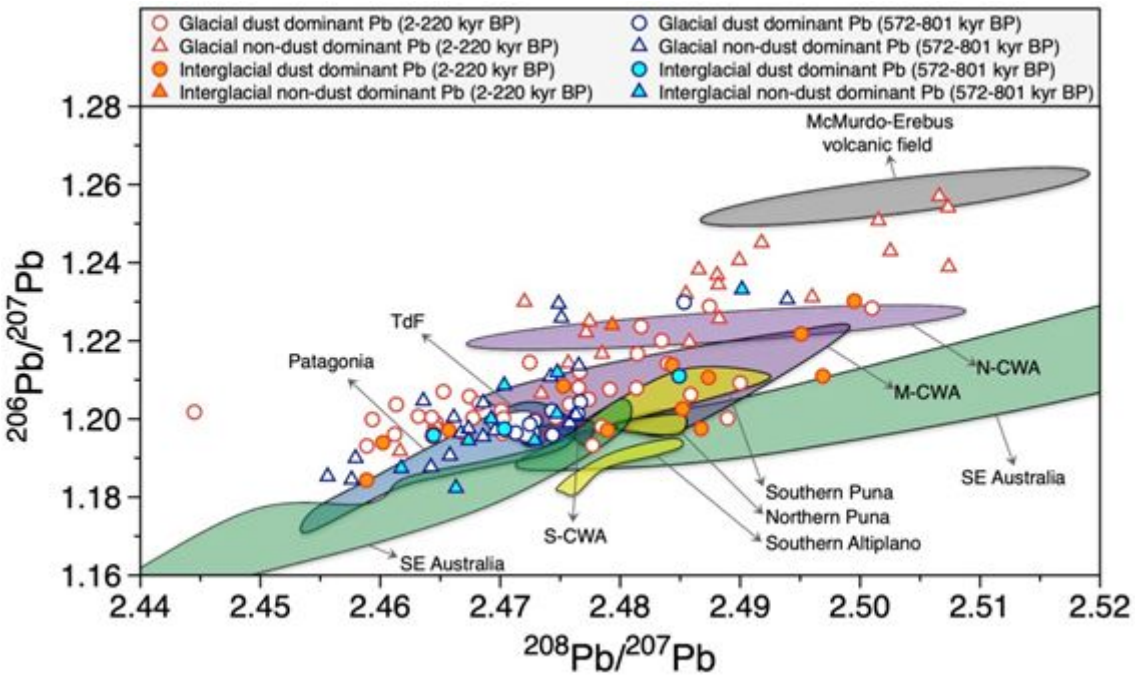

Figure 2

A plot of 208Pb/207 versus 206Pb/207Pb in the EDC ice core. Also included are data previously reported from the EDC ice core (shown in red)18. The isotopic fields of the potential source areas of dust and Antarctic McMurdo-Erebus volcanic sources were derived from the literature: Puna-Altiplano Plateau (PAP), central-western Argentina (CWA) and Patagonia/Tierra del Fuego (TdF)19, southeastern (SE) Australia (Murray-Darling Basin)18,30, and McMurdo-Erebus volcanics18.

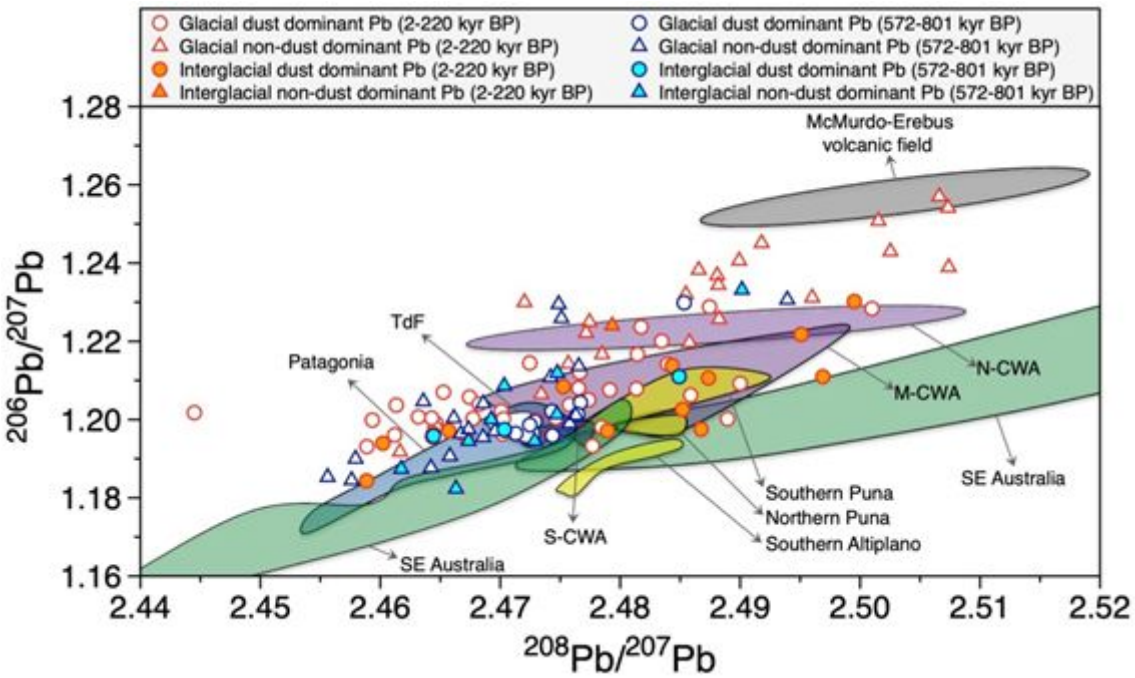

Figure 2

A plot of 208Pb/207 versus 206Pb/207Pb in the EDC ice core. Also included are data previously reported from the EDC ice core (shown in red)18. The isotopic fields of the potential source areas of dust and Antarctic McMurdo-Erebus volcanic sources were derived from the literature: Puna-Altiplano Plateau (PAP), central-western Argentina (CWA) and Patagonia/Tierra del Fuego (TdF)19, southeastern (SE) Australia (Murray-Darling Basin)18,30, and McMurdo-Erebus volcanics18.

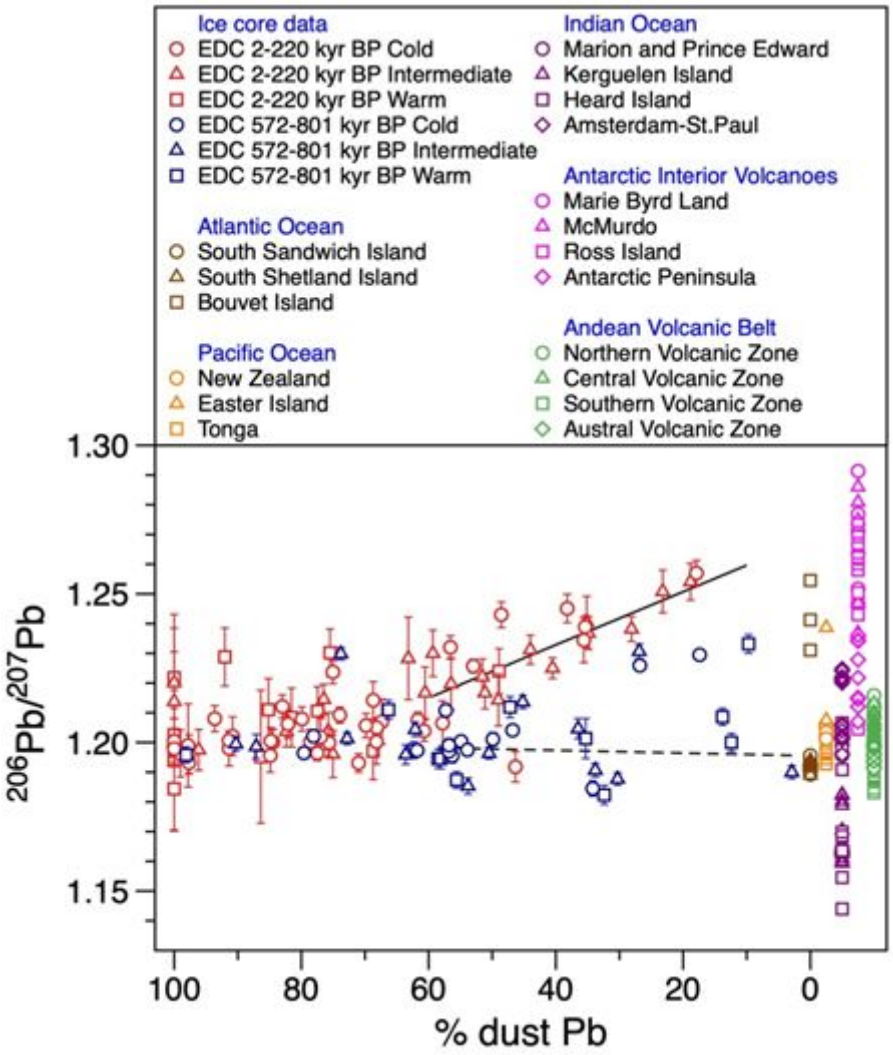

Figure 3

Comparison of 206Pb/207Pb ratios between the pre-MBE and post-MBE intervals as a function of the dust fraction of Pb in the EDC ice core samples. All uncertainties are 95% confidence intervals. The end-members of volcanic 206Pb/207Pb ratios for the potential volcanic sources come from published literature (see Figure S6). The locations of individual volcanoes are shown in Figure S7. Note that the fraction of dust Pb in excess of 100% shown in part of the post-MBE samples18 was considered to be 100%. The least squares lines are shown for the post-MBE (solid line) (Pearson's correlation of 0.717 at $p < 0.01$) and pre-MBE (dashed line) isotopic data (no correlation with Pearson's correlation of −0.088) with a dust-Pb fraction of < 60%. Four pre-MBE samples (nos. 20, 28, 29, 40) were excluded from any calculation because they are outside the general trend of the pre-MBE non-dust dominant isotopic compositions (see text).

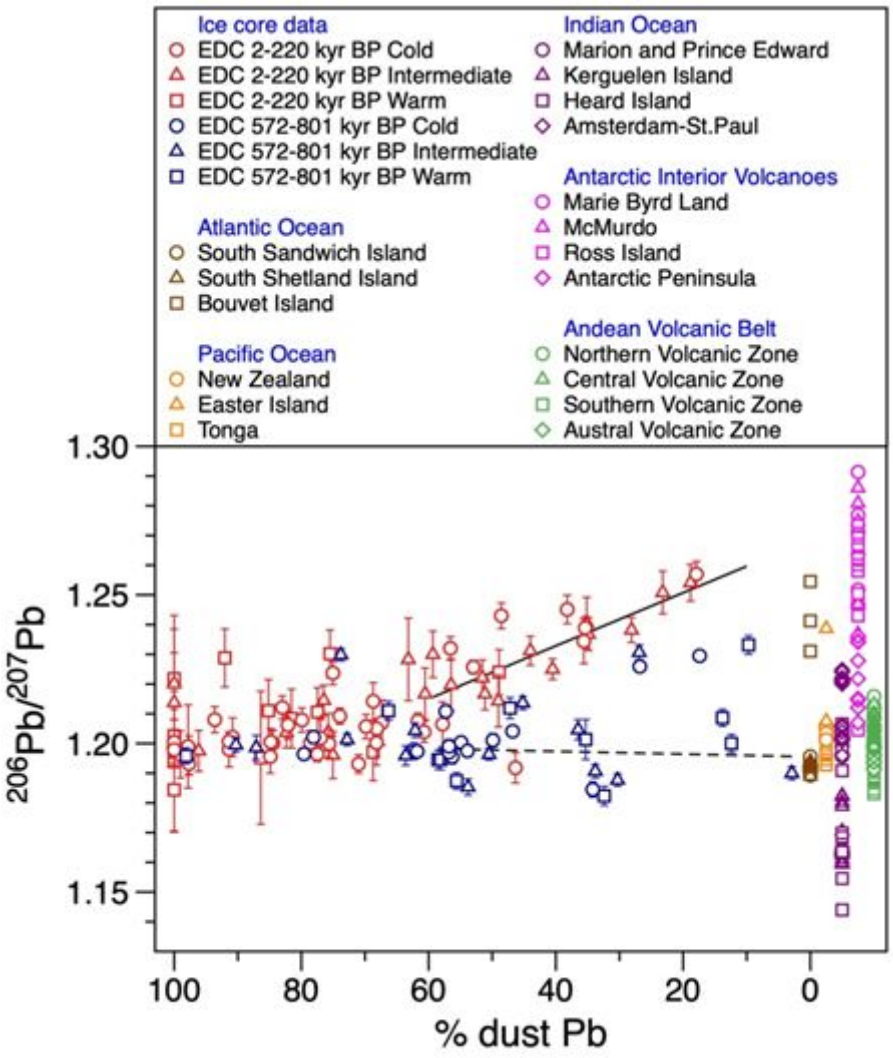

Figure 3

Comparison of 206Pb/207Pb ratios between the pre-MBE and post-MBE intervals as a function of the dust fraction of Pb in the EDC ice core samples. All uncertainties are 95% confidence intervals. The end-members of volcanic 206Pb/207Pb ratios for the potential volcanic sources come from published literature (see Figure S6). The locations of individual volcanoes are shown in Figure S7. Note that the fraction of dust Pb in excess of 100% shown in part of the post-MBE samples18 was considered to be 100%. The least squares lines are shown for the post-MBE (solid line) (Pearson's correlation of 0.717 at $p < 0.01$) and pre-MBE (dashed line) isotopic data (no correlation with Pearson's correlation of –0.088) with a dust-Pb fraction of < 60%. Four pre-MBE samples (nos. 20, 28, 29, 40) were excluded from any calculation because they are outside the general trend of the pre-MBE non-dust dominant isotopic compositions (see text).

Supplementary Files

This is a list of supplementary files associated with this preprint. Click to download.

- Supportinginformation20201201finalversion.docx
- Supportinginformation20201201finalversion.docx